Title
Divide-and-Conquer Chemical Bonding Models for Materials: A Tool for Materials Design at the Electronic Level

Journal
Chemistry of Materials, 29(20)

ISSN
0897-4756

Author
Alexandrova, Anastassia N

Publication Date
2017-10-24

DOI
10.1021/acs.chemmater.7b03138

Peer reviewed

Divide-and-Conquer Chemical Bonding Models for Materials: a Tool for Materials Design at the Electronic Level

Anastassia N. Alexandrova*

Department of Chemistry and Biochemistry, University of California, Los Angeles, Los Angeles, CA, 90095, USA, and [2]California NanoSystems Institute, Los Angeles, CA, 90095, USA

ABSTRACT: Chemical bonding, traditionally being the language of chemists, gives a wealth of intuitive shortcuts in understanding structure, properties, and reactivity of molecules. An analogous language based on structure or even just formula of materials would give tremendous advantage in materials discovery and rational tuning of their properties. The present perspective focuses on the "local", chemical approaches to rationalizing the chemical bonding in materials. The "divide" part of the approach consists of isolating relevant small fragments form the solid, either through electron localization schemes, or through directly considering small cluster fragments possessing bonding elements of the solid. The fragment is analyzed with state-of-the-art theory and experiment. Once the local bonding elements in the small unit and their relationship to structure and possible properties are realized, they get supplemented with energy content and mapped back onto the material, eventually enabling strategic modifications, and materials design. This constitutes the "conquer" part of the strategy. Several examples are presented when such chemical bonding analyses allowed the predictions of broader materials families than previously known. Discussed applications include surface alloys for catalysis, ultra hard bulk alloys, and 2D materials with interesting conductivities and magnetism.

1. INTRODUCTION

A chemical bond to a chemist is a model for interatomic interactions that is descriptive of the molecular properties, such as stability, reactivity, and structure/symmetry.[1,2] For example, given a Lewis structure, one can generally guess the approximate rotational barrier around a particular bond and know where to push an arrow in a scheme for a chemical reaction; lone pairs of electrons on atoms call for a hydrogen bond acceptor; aromaticity means high symmetry and specific reactivity. Obviously, these tools have been quintessential in chemistry, and central in the rational and speedy development of the field. Rather than every time solving the Schrödinger equation or performing

electronic spectroscopy, one can draw electronic structure and its consequences with a pencil in minutes, and easily communicate the material in an undergraduate class. No doubt a similar intuitive language would benefit materials research, and it could be a way to diminish the traditional empiricism in materials discovery.

However, chemists' view is molecular and local, and therefore, localization of the electronic structure is a bridge to build from materials to theory of chemical bonding, in order to use its fruits to the advantage of materials science. Some of the seminal and earliest views on the theory of chemical bonding in materials with a perspective of a chemist are owed to Linus Pauling[3,4] and Roald Hoffmann,[5] and several books summarize the developments.[6-8] In our view, the concept of local bonding in solids remained underappreciated, until several recent works on the rationalization and design of different types of materials have started giving the field its momentum.

The bonding analysis revealed the formation of molecular and local bonding features in compressed Li.[9] Local approach was shown to help rationalization of magnetism in materials, for example in the works of Goodwin, and Neilson. They showed that local distortions and covalency onset in disordered materials often govern materials' magnetism.[10] Magnetism in cobalt hydroxides, $Co(OH)_{2-x}(Cl)_x(H_2O)_n$, was explained through such a local approach.[11] The analysis of interstitial Mn in $Mn_{1+\delta}Sb$ showed that it if fruitful to consider distortions in the lattice away from crystallographic averages, and then the analyze the local bonding environment. The local atomic orbital (AO) overlap at Mn sites was shown to lead to perturbations in the local magnetic moment, and affect the resultant bulk magnetism.[12] These works are additionally beautiful for the fact that bonding is considered away from the equilibrium, and upon distortions relevant to realistic conditions of materials' applications. Local bonding models also help in rationalization and design for such properties as sorption and ion storage in aperiodic solids, where phonon coupling leads to the formation of local bonding motifs.[13] Consideration of local resonances and bonding is prominent in the works by Fredrickson.[14-16] His reversed approximation Molecular Orbital (raMO) method involves mapping the electronic structure of a material onto local MO diagrams to create Wannier functions, with the goal of tracing isolobal analogies. For example, in something as delocalized as BCC metals, as well as other more complex phases, the model recognizes the presence of localized d-AOs as well as metal-metal (M-M) bonds in resonance. The power of the model is in that the resultant understanding leads to predictions and design of new phases. Hole transport in doped NiO for

photovoltaic applications was shown to be local, and confined to certain directions in the lattice due to local magnetic couplings.[17]

Our own models of bonding in solids also belong to this class. We find bonding motifs that are local enough for chemists to recognize familiar patterns that can be associated with properties, but can be locally delocalized thus needing not to rely on resonance representations. We rely heavily on small cluster fragments isolated from the solid after considerations of localization patterns. This constitutes the "divide" part of the "divide-and-conquer" strategy. These clusters can be characterized with great care using both theory, and experimental spectroscopy. In this analysis, we can use the concepts from the theory of chemical bonding developed over the centuries in the chemistry community. From there, we can start understanding also the parent solids, which is the "conquer" part. In this article, we will demonstrate the utility of the approach and its predictive power for functional materials design. We will share a few example applications, such as heterogeneous catalysts, ultrahard alloys, and new 2D materials with interesting conductivities and magnetism. We hope our "divide-and-conquer" strategy to be a broadly applicable and chemically-intuitive for materials rationalization and design.

2. WHERE ARE THE BONDS IN MATERIALS?

Electronic bands of solids are delocalized, but delocalized bands do not necessarily mean delocalized bonding. Covalent materials certainly possess localized bonds in their usual sense, e.g. single C-C bonds in diamond. However, even for highly delocalized states in materials, more local bonding views may have their merit. Eberhart in his controversial yet exciting work on the Ag metal showed that perhaps any material can be considered as a collection of small fragments, or clusters (Figure 1).[18] He used the Quantum Theory of Atoms in Molecules (QTAIM), which analyzes the topology of the total charge density, ρ, and detects various topological features in ρ, such as critical points (CPs). When a single Ag atom is considered in the context of the infinite metal lattice (Figure 1A), ρ contains CPs on the atoms, bond CPs sitting on the bond paths and at the intersection with the zero-flux surfaces, and cage CPs or local minima in ρ. It is important that the language of QTAIM,[19] though alternative to molecular orbitals (MOs) or Lewis electron pairs, is also descriptive of the bonding. The amount of charge in a bond CP correlates with the bond strength, a curved bond path indicates electron excess or deficiency (i.e. delocalization), relative positions of CPs are important indicators of reactivity and possible reaction mechanisms, etc. In the Ag metal, a single Ag atom and

it first coordination sphere cut out of the crystal, result in the cluster, Ag_{13} (Figure 1B). ρ in the vicinity of the central Ag atom in this cluster exhibits large distortions as compared to the bulk. The boundaries of the central Bader atom are curved and converge at infinity outside of the cluster boundaries. The cage CPs are missing. Clearly this is not an adequate description of the state of a single atom in the metal. However, once the second coordination sphere is included, the topology of ρ becomes indistinguishable from that seen in the metal. Bond and cage CPs are in place, and the boundaries of the Bader atom are identical in the two cases, to a naked eye. Thus, QTAIM recovered a full description of chemical bonding in which Ag atom is engaged in the solid. This result is remarkable because we tend to consider metallic bonds fully delocalized, with all electrons belonging equally everywhere, and yet we see that in fact the bonding picture is very local, and is fully reproduced at the level of a small cluster fragment.

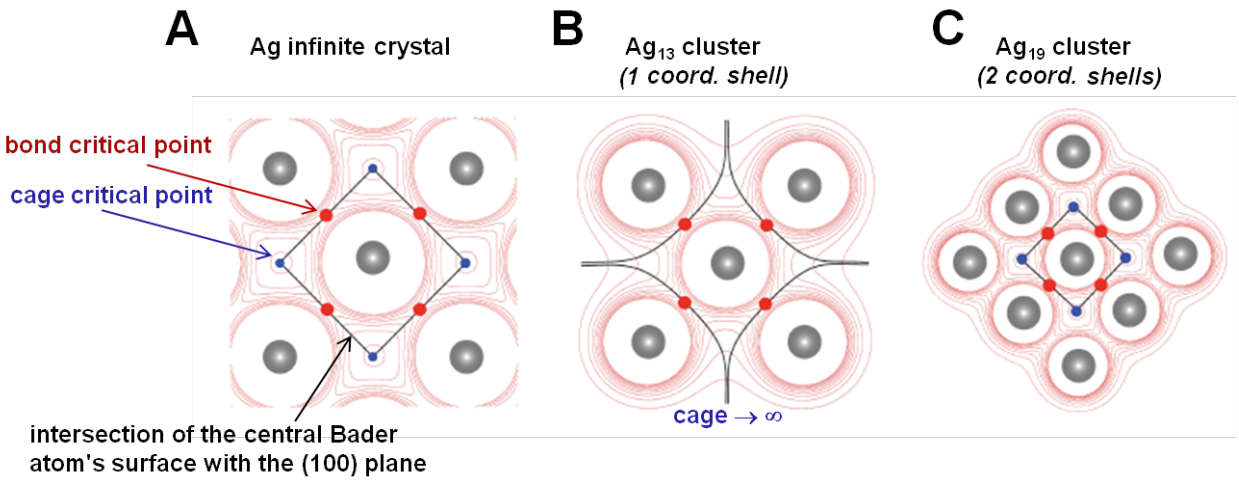

Figure 1. QTAIM view of the chemical bonding around a single Ag atom in (A) Ag metal, (B) Ag_{13} – cluster containing a single coordination sphere around the central Ag atom, and (C) Ag_{19} – cluster containing two coordination spheres around the central Ag atom. Bond CPs are in red, cage CPs are in blue. Notice the full recovery of the bonding picture once two coordination spheres are included. Adapted with permission from Eberhart, M. E. *Struct. Chem.* **2017**, DOI: 10.1007/s11224-017-0917-z.

Thus, small fragments can be adequately chosen to represent a material, though an algorithm is needed to make this choice physically-grounded. For fragments then, analysis can be done using all available chemical bonding tools, such as MO diagrams, electron localization functions (ELF),[20] or other bond localization schemes. The link between electron count, types of occupied orbitals, and structure/properties is much simpler to construct for a finite system. The fragment description has to

be mapped back onto the infinite material, and then we would finally arrive at the desired understanding at the level of functional materials design (by which we mean making rational choices for compositions via informed "short-cuts", and excluding approaches such as massive screenings and machine learning).

For the fragment-solid mapping to be predictive, however, one more ingredient is needed, and that is bond energy. Notice, for example, that, while the QTAIM description of Ag metal (Figure 1) gives a qualitative insight, and ρ in principle contains all the information about the system according to Kohn theorem, the connection between the geometry of ρ and such properties as stability and reactivity is largely hidden in QTAIM. For all but quite specific cases (e.g. dimers), QTAIM cannot be used to determine bond energies (i.e., the difference in total energy between a given state and a quantum mechanically ill-defined reference state), thus, for example, we cannot compare that energy to the energy of a reagent of interest, such as an intermediate in a catalyzed reaction. On the other hand, the language of molecular orbitals (MOs) contains the energy information, which translates to electronic spectra and reactivity. Hence, cluster fragments can be analyzed also via MOs. For molecules, through further electron localization via Natural Bond Order (NBO)[21] analysis or similar schemes, MOs can be converted to Lewis structures, if desired. Between MOs and Lewis, every chemist is comfortable in navigating the chemical space, drawing structures from molecular formulae, pushing arrows in chemical reactions, predicting the structures of reaction products based on the symmetries of the frontier orbitals, etc.

How can we localize bands and arrive to MO- or Lewis-like representation of materials? Localization schemes for extended systems that do not rely on resonances have been developed, and among them we would like to particularly highlight the Adaptive Natural Density Partitioning scheme, AdNDP.[22,23] This method is an extension of the already mentioned NBO, except that, in cases where the localization over one, two, or three atoms is impossible due to greater electron-deficiency, the method will proceed toward localizing electron pairs over more centers, but as few as possible. As a result, AdNDP recovers both "usual" Lewis-like bonding elements, and delocalized MO-like bonding elements, without invoking resonance. Avoiding resonance representation is attractive because it does not contradict the symmetry of the system. The price for the correct symmetry is the non-orthogonality of NBO and AdNDP orbitals or bonds, which, however, can be orthogonalized, if desired. This simple method gives a basic picture familiar to chemists, for any system, including inorganic solids. In Figure 2 we show examples of the applications of AdNDP to

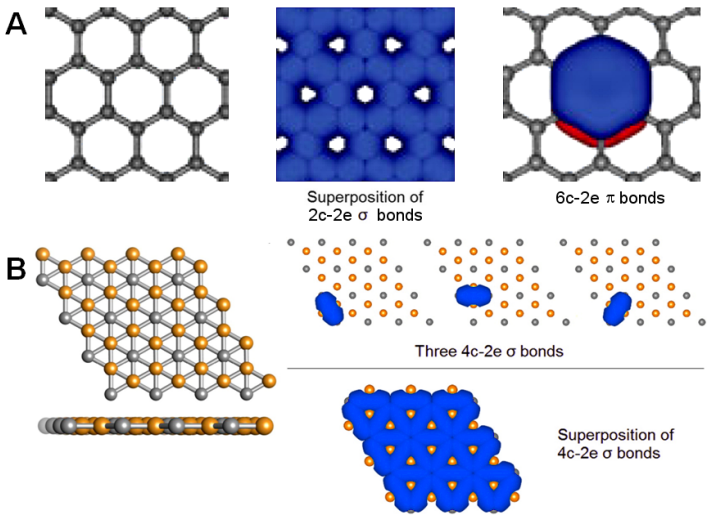

Figure 2. AdNDP descriptions of 2D materials: (A) graphene: classical 2c-2e C-C σ-bonds connecting all C atoms, and 6c-2e π-bonds, one over every C_6 ring, justifying local aromaticity of graphene. (B) The newly predicted 2D material, Cu_2Si (Cu – orange, Si – gray): apart from lone pair 3d-AOs on Cu atoms (not show), there are three symmetry-equivalent 4c-2e delocalized σ-bond, one per Cu_2Si_2 unit (shown individually, and then superimposed) that bond the material together. This material has no π-bonding. Adapted with permissions from Popov, I. A.; Bozhenko, K. V.; Boldyrev, A. N. *Nano Research* **2012**, *5*, 117-123, and Yang, L.-M.; Bačić, V.; Popov, I. A.; Boldyrev, A. I.; Heine, T.; Frauenheim, T.; Ganz, E. *J. Am. Chem. Soc.* **2015**, *137*, 2757-2762.

extended solids, graphene[24] and newly predicted Cu_2Si.[25] AdNDP shows that, in graphene, there are first of all single C-C σ-bonds, just as we would draw intuitively. The π-system of electrons can be maximally localized in such a way that one electron pair would belong to every C_6 ring. This is different from benzene that has 6 electrons per C_6. Based on the (4*n*+2) Hückel's rule for counting delocalized electrons, graphene is therefore locally π-aromatic with *n*=0. Cu_2Si (Figure 2B), despite having a 2-D structure and relatively high stability, is not held together by π-bonding. Instead, the material contains delocalized 4c-2e bonds over sets of 2 Cu atoms and 2 Si atoms.

This localization protocol is consistent with the symmetry of the system, and relates to the general chemistry knowledge, such as electronic count in aromatic systems. One aspect that is not reflected in the AdNDP representation, however, is the connection to properties, such as reactivity or conductivity. For example, one would not be able to conclude from AdNDP that graphene is a zero-band gap semiconductor, and Cu_2Si is a metal. Intuitively, localized C-C σ-bonds in graphene should be "more local" than 6c-2e π-bonds, which (as is known) belong to very steep π-band that touches E_F at the tip of the Dirac cone. AdNDP does not relate to such energy information by design, because it transforms the electronic states away from their eigen-meaning. Lewis structures in organic

chemistry also lack the energy content, and, in order to arrive to Lewis representation computationally via NBO, we also scramble the Fock matrix whose eigenstates have the meaning of Koopmans' theorem. Nevertheless, from years of experience, particularly in organic chemistry, we have the energy information in the back of our minds, and do not need it to explicitly come out of the Lewis model. For example, we know that C-C σ-bonds in molecules are stronger and have lower energies than π-bonds, and therefore have different reactivity; we can identify good hydrogen bonding partners, or back-donation schemes in organometallic chemistry, etc. Can we develop a similar intuition about energies of states in solid state? We probably cannot, because materials encompass a much broader chemical space, with many complex and exotic phases, making it hard to keep the energy relationships between various bonding elements at our fingertips. Even in the simple 2D solid made of C, graphene, the AdNDP-ascribed local π-aromaticity (Figure 2A) does not have the same meaning as π-aromaticity in benzene. The fully-bonding 6c-2e π-state in graphene is near E_F, but in C_6H_6 it is far below the HOMO-LUMO gap. Hence, even though these π-states look the same, for benzene we would not suspect it to participate in electronic conductivity, or undergo an electrophilic attack, but for graphene – we would. Therefore, AdNDP shows us that a given state exists and does not conflict with the symmetry of the system. It is a convenient picture for chemists. To some extent, relying on AdNDP analysis, and we can make predictions about structural changes upon modest changes in composition. However, we do not generally know how to translate AdNDP information to chemical and physical properties. Also, for competing polymorphs, AdNDP can produce bonding schemes that are consistent with each structure, but this analysis would not tell us which phase should have lower energy. It would be good to put the energy information back in connection with AdNDP or another localized bonding representation, to have a visual, intuitive, and predictive bonding picture that chemists could use for property design in materials.

In this vein, our approach has been based on small cluster models, probed theoretically and also often experimentally, and chosen on the basis of the features of the electron density in the bulk material, obtained with ELF,[20] QTAIM, AdNDP, or another method. Small clusters can be interrogated with high-level wave function based theoretical methods, which are inaccessible for solid state, and that is often crucial for explaining properties of the bulk. Precision gas phase spectroscopy is also possible. The mapping of the electronic structure of the cluster model back onto the solid is done via a combination of cluster MOs, and material band structure, both of which are associated with eigenenergies. Occasionally, we use the AdNDP representation directly. In those

cases, density of states (DOS) projected on AOs can be linked to the linear combinations of AOs constituting AdNDP states, and in this way we re-link AdNDP to energies. We do not invent a completely new technique, but we combine the localized bonding picture and the energy information in such a way that it becomes intuitive for chemists, and rationalization and prediction of functional materials actually becomes possible. Details and examples are presented in the sections below.

3. ENERGY-INFORMED CLUSTER-BASED APPROACH TO BONDING ANALYSIS IN MATERIALS AND MATERIALS DESIGN

3.1. Locally aromatic catalytic surface alloys and 2-D materials. We will start from the surface alloys: borides, carbides, and nitrides, of Co and Ni.[26] These materials are important in catalysis. Carbon embedding in the surfaces of the Co and Ni metals initiates coke deposition and eventual blocking of all sites on the metal and poisoning of the catalysis, Co – in Fischer-Tropsch synthesis, and Ni – in steam reforming. Coking is a great problem, which industrially causes the need for a costly catalyst recovery. It was discovered that boration of Co and Ni prior to the catalytic reaction extends the life-time of the catalysts.[27,28] Apparently, boron binds the carbon binding sites on these surfaces, and does so more strongly than carbon, while minimally modifying the electronic properties of the metal. Thus, the coking initiation step is halted, while catalysis done by the metal is still possible. The questions that we initially asked where the following: Why do boron and carbon bind to Co and Ni so strongly, despite the anomalous square-planar coordination? Why does main-group element binding cause the p4g surface reconstruction (Figure 3A)? Finally, why does B have the special ability of outcompeting C in binding and yet keep the metal catalytic?

In the DOS plot for the reconstructed Ni_2C surface alloys shown in Figure 3B, we see a sharp peak marked with a dashed line. Here, the states responsible for binding C are segregated. The sharpness of the peak indicates localization. The inset shows the charge density in this region, which is clearly localized primarily on C. The Bader analysis of the charge distribution in the surface alloy indicates that C is anionic, and the metal is cationic, while the slab beneath the top monolayer remains virtually neutral, i.e. unchanged from the bulk metal. Thus, the bonding between the metal and C is confined to the top monolayer. Furthermore, a Ni_4C^+ cluster cut out of the surface alloy and placed in the sea of charges positioned as in the alloy lattice has the same charge distribution: anionic C, and Ni holding a +0.5 charge. Therefore, the M_4X unit, M=Co,Ni, X=C,B, in the surface

alloy (Figure 3A) is a representative cluster that should contain the localized bonding elements responsible for strong binding of C/B, in the unusual square planar configuration.

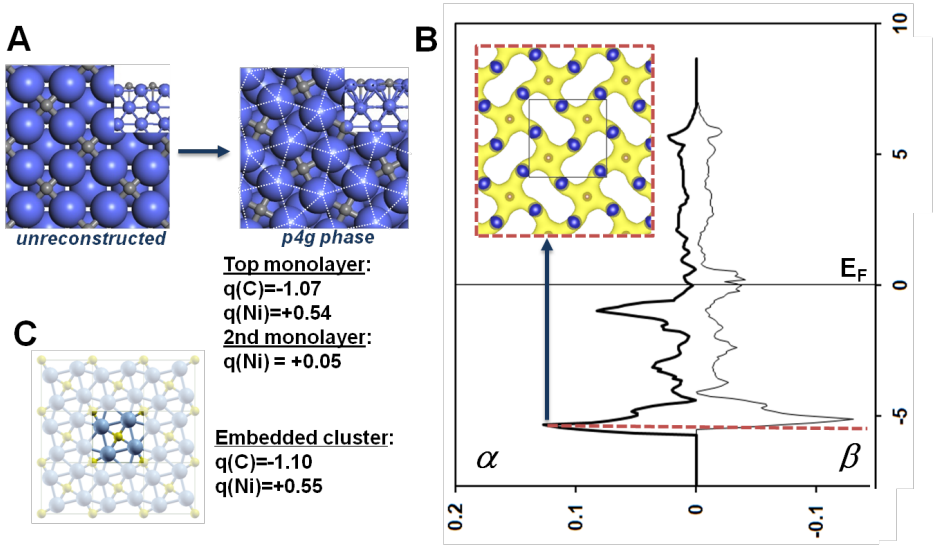

Figure 3. (A) C (as well as B) bind to Ni and Co in ½ ML coverage, and cause the spontaneous p4g reconstruction. Ni – blue, C – gray. (B) The DOS plot for surface Co_2C. The peak indicated with a dashed line corresponds to the states responsible for binding C to Ni. The peak is sharp, indicating localized states, and this is additionally supported by the plot of the electron density in the inset, corresponding to the position in DOS indicated by the dashed line. (C) A Ni_4C^+ cluster embedded in the sea of charges provided by the bulk has the same charge distribution as does the Ni_4C unit in the bulk surface alloy shown in (A). Adapted with permission from Nandula, A.; Trinh, Q. T.; Saeys, M.; Alexandrova, A. N. *Angew. Chem. Int. Ed.* **2015**, *54*, 5312-5316.

In our original publication[26] we simply analyzed the delocalized wave functions of the surface alloy to draw our conclusions. However, we subsequently further supported the conclusions through the AdNDP analysis. Selected results from AdNDP are shown in Figure 4C:[29] these are the maximally localized states that involve the bound main group element. All of them have good occupation numbers (ON) (close to 2, for an electron pair). The schemas in the bottom row in Figure 4 show the AO-overlaps responsible for the formation of the AdNDP states. There is a set of 3 σ-states formed by the in-plane overlap of the $3d_{xy}$-AOs on M and the 2s-, $2p_x$-, and $2p_y$-AOs respectively on X. These are delocalized 5c-2e bonds. Containing 6 electrons, they make the system obey the (4*n*+2) Hückel's rule for aromatic compounds, with *n*=1. Therefore, we can call the M_4X unit locally σ-radially aromatic. One other 5c-2e σ-state is of the peripheral type, as it involves the AO-overlap along the periphery of the 4-membered cycle. The state is formed by the d_{x2-y2}-AO on the metal, with a minimal involvement of the high-energy 3d-state on X (interestingly, the 4c-

localization that would not involve X but only M_4 was not achievable). 2 electrons populating this delocalized state again obey the (4*n*+2) Hückel's rule with *n*=0, and make the system also σ-peripherally aromatic. Finally, there is a single π-aromatic state formed by the $2p_z$-AO on X and $3d_{xz}$- and $3d_{yz}$-states on M. Thus the local M_4X unit is triply-aromatic.[28,29] We note that we base the notion or aromaticity purely on the Hückel's style electron count. Aromaticity is nothing more than a term for the delocalized bonding situation where there is an even population of degenerate electronic states, which therefore preserves the symmetry. Another way to assess aromaticity is by calculating the resonance stabilization energy, which, however, is not trivial for solid state. Multiple other criteria of aromaticity and its degree exist in the literature, but we feel no particular need for them, as the most traditional electron count has not ever failed yet (unlike, for example, NICS indices).

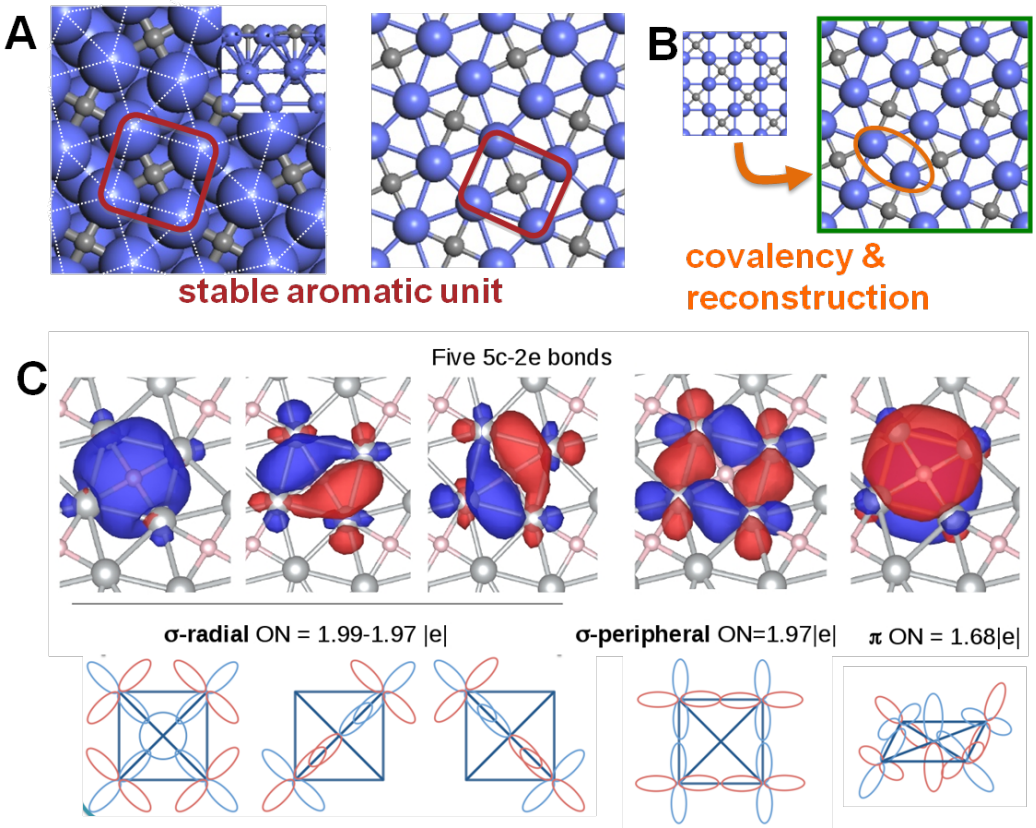

Figure 4. (A) The surface borides, carbides, and nitrides of Co, Ni and few other metals were discovered to have an unusual and yet very stable structure, with square planar coordination of the main group element and p4g reconstruction. The structure persists in 2D carbides and nitrides of Co and Ni. (B) The spontaneous p4g reconstruction is driven by the disruption of the bonding between the top monolayer and the bulk phase beneath, and the formation of the covalent M-M bond across the void. (C) The AdNDP electron localization analysis showing the delocalized 5c-2e bonds and multiple aromaticity in the M_4X (X=B,C,N, M=metal) unit, with the schematic MO-LCAO representation given below. The local aromaticity explains the stability of XM_4. Adapted with

permission from Nandula, A.; Trinh, Q. T.; Saeys, M.; Alexandrova, A. N. *Angew. Chem. Int. Ed.* **2015**, *54*, 5312-5316.

In fact this bonding picture is very similar to what has been observed in the gas phase Al_4C^- cluster, characterized by theory and photoelectron spectroscopy.[30,31] The cluster is also square planar, and was defined as triply-aromatic. The only difference is that Al uses its 3p-AOs for the overlap with the 2s- and 2p-states of C, instead of the 3d-AO in Co and Ni, but the structure and symmetry of the resultant delocalized MOs is the same as in Figure 4. Many other molecular square-planar C systems have been reported as well.

What is the use of calling the M_4X unit aromatic? Aromaticity in chemistry is a phenomenon associated with high symmetry, stability, and specific reactivity (unwillingness to engage in reactions of addition that break aromaticity). For chemists, aromaticity is a "short-cut" view on the electronic structure, a way to immediately see the chemistry that follows. Indeed, in our surface alloys, the aromatic arrangement is exceptionally stabilizing. This can be seen in multiple ways. First of all, again, the X-binding states lie deep below E_F (Figure 3). Our localized AdNDP states directly correspond to these delocalized states of the solid, as can be proven by finding them among the true plotted wave functions across the Brillouin zone,[26] or via DOS projections on AOs. Secondly, tetracoodinated C is usually tetrahedral, sp^3-hydridized, and participates in 4 covalent bonds. However, in our alloys, C forgoes the usual drive for hybridization (notice that in all states C contributes s- or p-AOs, or nothing, but never a sp-mix, as the mixing is forbidden within the D_{4h} point group), and instead goes anionic, allowing for the aromatization of the M_4X unit. Apparently, this is energetically more beneficial than going sp^3. Lastly, as a tribute to the stability of the aromatic arrangement, we showed that upon replacement of M and X (M = Co, Ni, Cu, Rh, Pd, Ag, and X = B, C, N), the states that bind the main group element remain exactly the same.[26] The alloys hold onto their triply-aromatic coordination of X, even though the charge distribution may vary drastically, e.g. B is nearly neutral, while C has the charge of -1. Notice additionally that, while some of the 3d-AOs are used to bind the main group element, most of them stay intact and metallic, which is why borides (and also carbides before the surface is fully coked) are still catalytic. Hence, we have at hand the intuitive localized bonding picture linked to the energy characteristics. It can be used as guidance for further reactivity arguments, for example, through comparison of the energies of X-binding state to the frontier MOs of molecules, such as reaction intermediates in a catalytic process.

The chemical composition of M_2X affects the overall material's stability, such that less electron-rich alloys are more stable, and also undergo a stronger p4g reconstruction. The reconstruction consists of decreasing the angle between the two squares binding X, closing the bond across the diagonal in the void square. It was found that, as the number of electrons reduces upon progressing from Cu/Ag to Ni/Pd to Co/Rh, and from N, to C, to B, the number of occupied antibonding states across that diagonal reduced. Hence, the M-M bond becomes stronger and shorter, and the materials reconstruct more strongly, gaining stability through bond formation. Notice that the chemical term of local covalency carries a clear message for chemists. It indicates stability gained through the formation of an electron pair. It is thus clear why Co and Ni borides are more reconstructed and more stable than the corresponding carbides, and why boron prevents coking on these surfaces. The discovery of B as a useful dopant was made in the catalysis community accidentally and without much rationale. Now, we hope that, given the renationalization of the effect, the bonding principle will help in the future selective catalyst design.

Notice that through the study just presented, we not only rationalized structures and the electronic origin of the effect of B on the selectivity of catalytic processes, but we also predicted a new family of surface alloys, beyond carbides and borides of Co and Ni, all of which are stabilized by the same bonding pattern.

Taking one step further, we recall that the slab beneath the top monolayer in the studied surface alloys remained electronically identical to the pure metal, i.e. it did not participate in binding the main group element. That suggested a possibility that the top monolayer could be lifted off of the slab, and retain the bonding pattern and stability. It turns out that the binding energy to the slab below is still rather high, due to the M-M bonds between them. However, if the aromatic monolayer is put epitaxially on top of a metal with a slightly different lattice constant, e.g. Ag for Co and Ni carbides/nitrides, then the exfoliation costs only a few or a fraction of kcal/mol.[29] Hence, there is a possibility of preparation of such 2-D materials. Carbides and nitrides of Co and Ni (Figure 5) were predicted in this way, while borides adopt 3-D structures when exfoliated and relaxed. The carbide and nitride monolayers are calculated to have no imaginary phonons. Additionally, they retain their structure and aromaticity up to striking 1,800 K, according to Born-Oppenheimer Molecular Dynamics (BOMD). They are definitely metastable phases, but obviously highly kinetically trapped. The interesting property of these 2D carbides and nitrides is that they are still metallic. Just like in the surface alloys, some of the d-electrons of the metal got consumed for bonds with C/N, but other

d-states remained metallic and close to E_F. Furthermore, the Co system also retained magnetism: the ferromagnetic phase is more stable than antiferromagnetic or those with intermediate total spins. To the best of our knowledge, magnetic 2-D alloys are exceptionally rare, and therefore should be of broad interest. The predicted 2-D materials wait to be experimentally realized and tested.

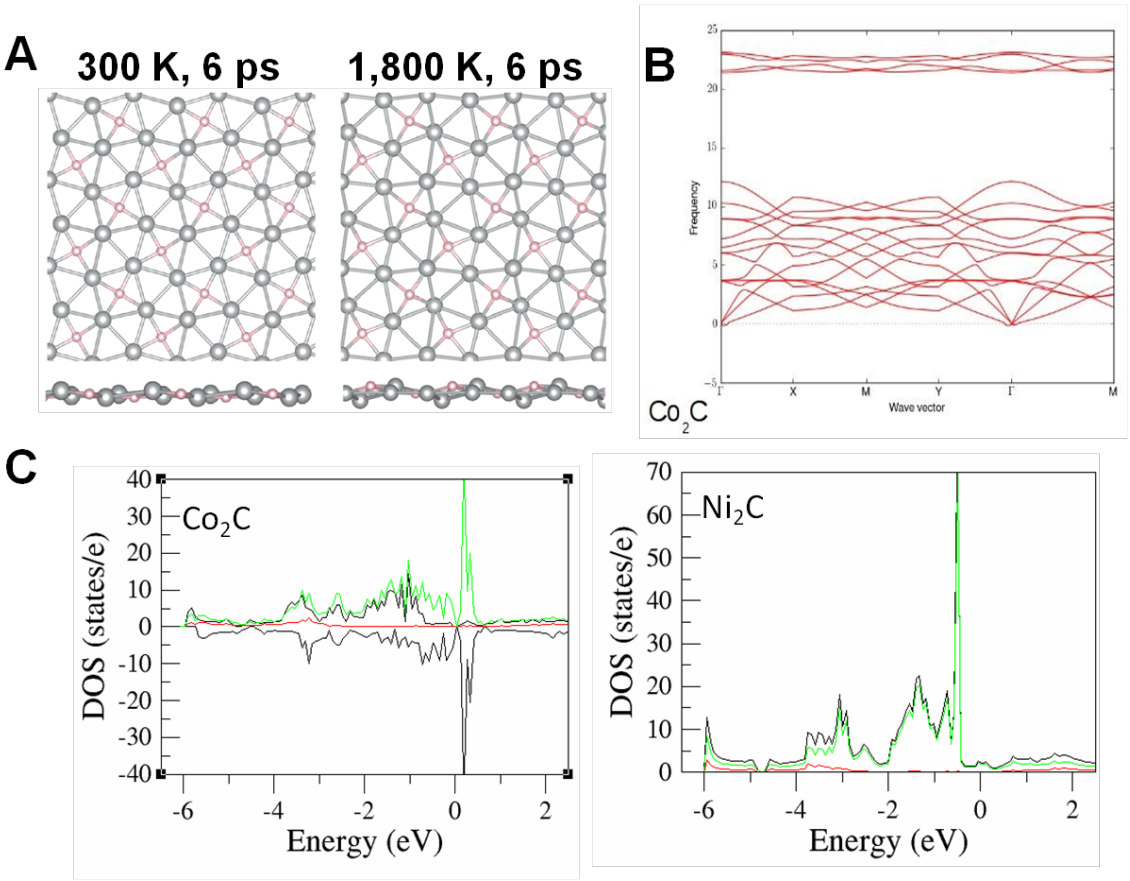

Figure 5. (A) Stable locally-aromatic 2-D carbides and nitrides predicted: structures are the same as those of the top monolayers of the surface alloys, and are retained up to 1,800 K, only subject to minor buckling, according to BOMD. (B) No imaginary phonons are found. (C) The materials are metallic, and Co alloys are also magnetic (DOS are shown for carbides only). Adapted with permission from Jimenez-Izal, E.; Saeys, M.; Alexandrova, A. N. *J. Phys. Chem. C* **2016**, *120*, 21685-21690.

3.2. 3-D borides: link between bonding and hardness

Ultra hard materials are of interest since prehistoric times. Until recently carbides were generally used for hard tools, though they are not superhard according to Vickers Hardness criteria, ≥40 GPa. Diamond and cubic boron nitride are the hardest materials known, but are very expensive as their production necessitates high *T* and *P*. Additionally, diamond easily forms carbides with ferrous metals at high *T*, further limiting its utility in machining. Another challenge comes in cutting super

hard materials. The recent invention of superhard metal borides is an exciting new route to superhardness, potentially free of the limitations of diamond-like materials.[32-35] Some borides of heavy transition metals can scratch diamond in certain crystallographic orientations. Most d-electrons in these materials remain purely metallic, so the materials are electrical conductors. Thus, they are easily cut with electric discharge machining (EDM), facilitating practical use.

Materials of this group are puzzling in many ways, and most disheartening is the fact that we so far have no way to predict which particular boride is going to be superhard. Borides are interesting structurally, as boron networks in them can adopt a variety of shapes: chains, sheets, or cages, and sometimes they have extreme stoichiometries, such as YB_{66}.[36] Some borides bring surprises, such as high-Tc superconductivity,[37] exotic magnetism,[38] topological and Kondo insulator properties,[39,40] unusual bonding motifs,[41] novel coordination chemistry,[42] and catalytic properties.[27,28,43-46]

With the goal of rationalizing borides, and predicting new ultra hard ones, we studied several of them, and probed their chemical bonding in equilibrium and under stress, as well as hardening via for example formation of solid solutions. Here, we will discuss a group of three borides, which are stoichiometrically identical, structurally similar and yet distinct, and very different in hardness: TiB_2 (25 GPa), ReB_2 (37GPa), and OsB_2 (21GPa) (Figure 6A).[47] All of them contain boron sheets, flat in TiB_2, bent as a "chair" in ReB_2, and bent as a "boat" in OsB_2. The questions that we aimed to answer are: Why is there a structural difference? Why is only ReB_2 superhard? Can we use the understanding of the electronic structure differences in these three borides to predict trends in hardness of other materials of this family, including solid solutions?

We start from the realization that, contrary to the older interpretations, borides feature metal-boron (M-B) bonding, and not just contain a separate boron sub-lattice. In all three structures, M interacts with the boron network by facing a B-B unit (though in OsB_2 there are two inequivalent B-B bonds, a short and a long one). Therefore, we begin from small cluster models, $TiB_2^{0/-}$, $ReB_2^{0/-}$, and $OsB_2^{0/-}$ (Figure 6B,C). The anions are also studied because we probe them both theoretically and using photoelectron spectroscopy (Figure 6C), and the agreement between computed and experimental spectra allow us to conclude that our theoretical methods can inform on the bonding motifs available in the clusters. One important feature of the boron dimer is that the LUMO is a bonding σ-MO formed by $2p_x$-AOs. As a result, when transition metals interact with B_2, they back-donate not to a σ*-MO (as in the case of C-H or C-C), but to the bonding σ-MO, thereby making the B-B bond stronger, not weaker. The $\sigma(3d_M \rightarrow \sigma(LUMO)_{B2})$-MOs are present in all three clusters

(outlined in red, in Figure 6B). However, in $ReB_2^{0/-}$ and $OsB_2^{0/-}$ these states fall deep below the HOMO-LUMO gap, signifying strong covalent overlap between the metal and boron. In $TiB_2^{0/-}$, the

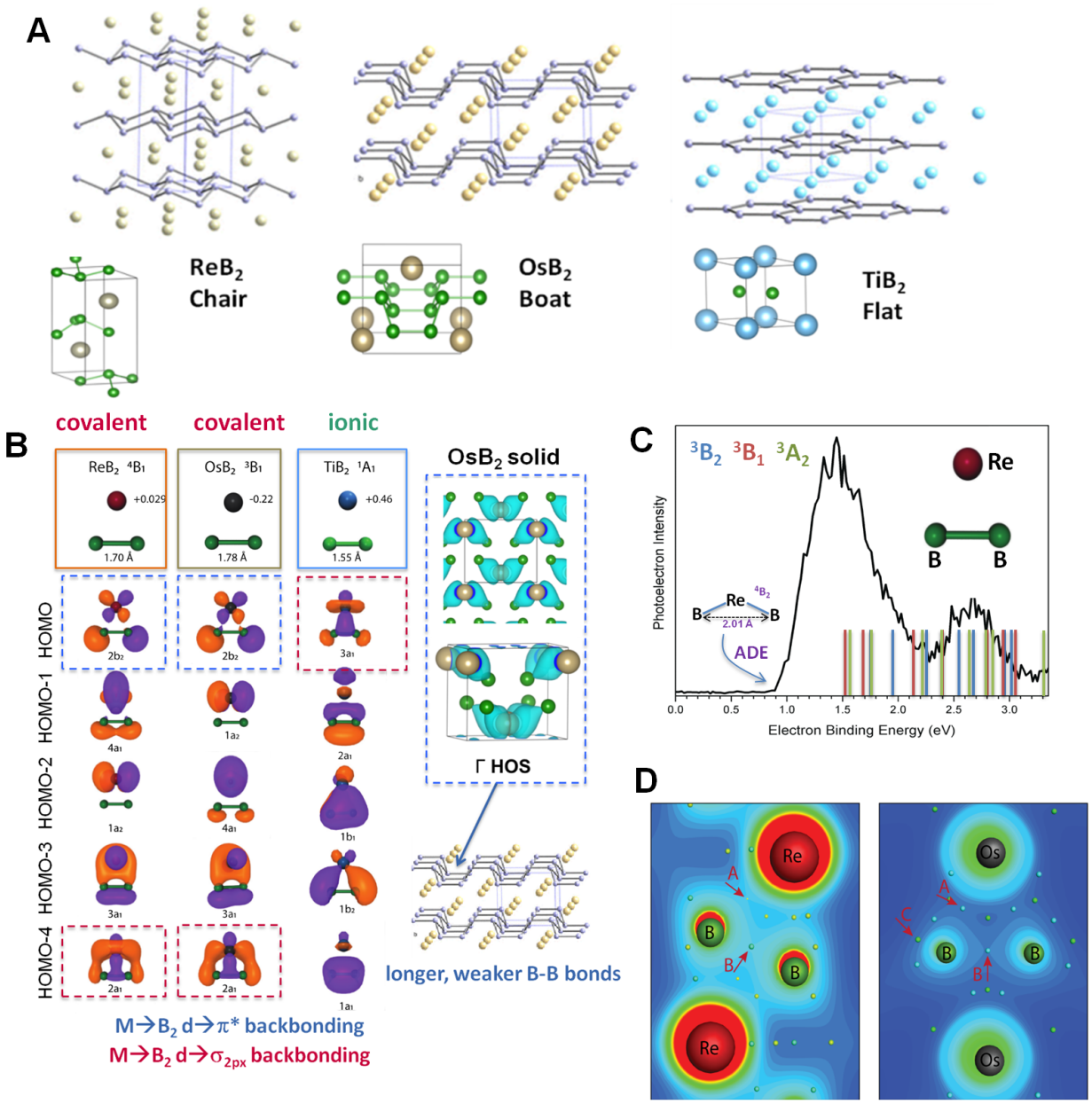

Figure 6. (A) Three structurally similar yet distinct borides with very different hardness: the bulk structure. (B) The small cluster models, ReB_2, OsB_2, TiB_2, that illustrate the bonding present between the metals and boron network in the three borides, with their valence MOs; the covalent $3d_M \rightarrow \sigma$ interactions are outlined in red; the $3d_M \rightarrow \pi^*$ states (outlined in blue) are higher in energy and irrelevant in the bulk. The MOs covered by the blue panel are present in the undercoordinated clusters but not in the fully coordinated solid. (C) Photoelectron spectrum and its theoretical interpretation for ReB_2^-, supporting theoretical description of the cluster. (D) QTAIM view on the M-B and B-B interactions in the ReB_2 and OsB_2 solids; A, B, C are bond CPs. The amounts of charge in these CPs are given in Table 1.

$\sigma(3d_M \rightarrow \sigma(LUMO)_{B2})$-MO is the HOMO. In addition, both Re and Os are capable of interacting with the LUMO+1 (π^*-MO) of B_2. The resultant state is the HOMO in both clusters. It strengthens the M-B bonding, and weakens the B-B bond. Thus, $ReB_2^{0/-}$ and $OsB_2^{0/-}$ have a strong covalent character of M-B bonding, and $TiB_2^{0/-}$ has a weaker covalent character.

Atoms in clusters are valence-undersaturated as compared to atoms in the solids, and therefore the upper-most MOs are not going to have analogues among the occupied states in the bulk. Specifically, the $d \rightarrow \sigma$ M-B backbond is unoccupied in TiB_2, and the material therefore retains only ionic bonding between boron and the metal. The charge on Ti is very close to +2 indeed, giving every B atom one extra electron. B^- is isoelectronic to C, and the boron sheet is therefore isoelectronic and isostructural to graphene. In ReB_2, the $d \rightarrow \pi^*$ state (the HOMO in the cluster) is unoccupied, whereas the $d \rightarrow \sigma$ M-B backbond is occupied. Thus, there is a covalent character to the Re-B bonding in the solid, reflected in the charge on Re of +0.39. Importantly, the $d \rightarrow \sigma$ backbond strengthens both the Re-B and the B-B bonding. OsB_2 also has the $d \rightarrow \sigma$ state occupied in the bulk. However, having one electron more than Re, it also keeps partial occupation of the $d \rightarrow \pi^*$ backbond, between Os and the longer (activated) B-B bonds in the solid (Figure 6B). Hence, OsB_2 has the highest M-B covalency, and a combination of stronger and weaker B-B bonds due to the interactions with the metal. Os is also nearly neutral, according to Bader charge analysis. Another proof of stronger covalency of the M-B bonds, and relatively weaker long B-B bonds in OsB_2 as compared to ReB_2 was generated using QTAIM (Figure 6D, Table 1). CP_A, CP_B, and CP_C are bond CPs corresponding to M-B bonds, and two types of B-B bonds, respectively. The amount of charge in bond CP is indicative of bond strength. We see (Table 1) that even though both borides have covalent component to the M-B bonding, Os forms more covalent interactions than Re does, both in the parent and the substituted boride structures. In the boat structure, half of the B-B bonds are weaker than Os-B bonds. Hence, stronger M-B interactions in OsB_2 take the charge density from the boron network, effectively weakening it.

There transpires a correlation between the covalency of M-B bonding and hardness. To pin it down, we subjected the clusters and solids to mechanical deformation stress: compression and shear (Figure 7), the combination of which jointly reports on material hardness. We see that, being purely ionic, TiB_2 yields most easily to the shear deformation (it slides). OsB_2, with most covalent M-B

interactions resists shear the most. ReB_2 is in-between. The compression, on the other hand, is the hardest for TiB_2, where no electron flow toward Ti-B bonds can relieve the electron-rich B-network. OsB_2 is the softest to compression, because of electron delocalization between Os-B and activated B-B bonds. ReB_2 is again in-between. Hence, while TiB_2 yield to shear, and OsB_2 yields to compression, ReB_2 does not easily yield to either of these stimuli. It is clear that the specifics of the local M-B bonding are responsible for the effect. Re has just the right electron count to have d→σ states populated but d→π* states not populated. As a result ReB_2 is the only ultra hard boride in the set. Finally, we tested the model by making a solid solution of Os and Re borides. As expected Os makes the ReB_2 structure less hard, and Re makes the OsB_2 structure harder.

Hence, with the help of intuitive cluster models where all bonding interactions are clear, we learn which types of M-B interactions are crucial for hardness. This is a new word in the theory of boride hardness, which until now ignored M-B interactions.

Table 1. Charges at bond CPs (shown in Figure 6D) in the Os and Re borides in their parent structures and substituted into the structure of the other metal. The differences between the amount of charge in the B-B bond across borides, and in the M-B bond(s) across borides illustrate the relative degrees of covalency in those bonds.

	CP_A(M-B)	CP_B(B-B)	CP_C(B-B)
ReB_2 boat	0.608 e^-	0.740 e^-	0.697 e^-
OsB_2 boat	0.656 e^-	0.732 e^-	0.618 e^-
ReB_2 chair	0.590 e^-	0.713 e^-	
OsB_2 chair	0.629 e^-	0.668 e^-	

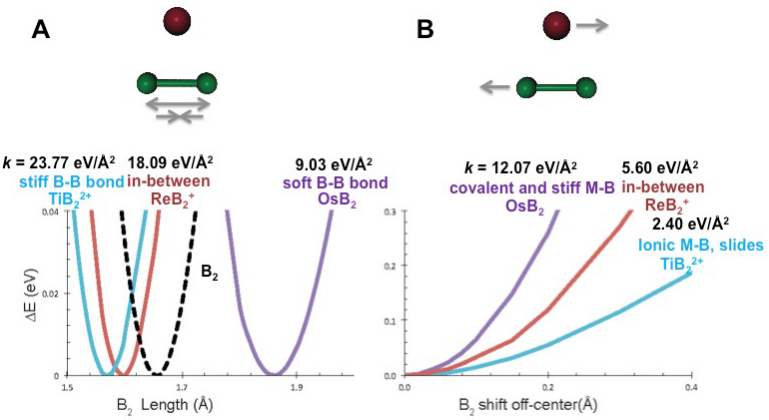

Figure 7. (A) Energies of the clusters as a function of (A) compression along the B-B bond, (B) shear distortion coordinate. Cyan - TiB_2^{2+}, Red - ReB_2^{+}, Purple - OsB_2 (charges are chosen to represent the occupation of the electronic states in the solid), dashed black - isolated B_2.

3.3. 2-D boron and conductivity

Given the excitement around 2-D carbon, a hunt for 2-D boron has been intense. Planarity does not easily come to the extended boron systems, because of its electron-deficient nature as compared to carbon: like a metal, the metalloid boron tends to go toward 3D bulk. In purely theoretical works, a large amount of effort went into finding stable 2D boron phases, e.g., the α sheet,[48,49] β sheet,[48,49] and χ sheet.[50,51] One phase was even predicted to be superconducting.[52] It was realized that truly atom-thick boron sheets can be grown on metal supports, and possibly eventually exfoliated to give a metastable phase. The underlying metal lattice plays an important role in defining the morphology of the phase. Subsequently, a few types of boron sheets been synthesized on Cu foils[53] and on a Ag(111) surface[54,55] by chemical vapor deposition (Figure 8A).

We predicted another, and very interesting phase of 2-D boron to form on W(110) (Figure 8B).[56] It consists of the ribbons of conjugated B_6 rings each filled with another B atom, and ribbons of conjugated B_4 rhombuses, with single bonds linking the two types of ribbons in the sheet. The search was done using an automated global optimization algorithm. We named this phase a π-phase, for reasons to be explained shortly. W(110) has rectangular lattice instead of hexagonal like those of Ag and Cu, and that defines a new structure of stable 2-D boron. The π-phase is nearly planar on W(110), and becomes completely planar when lifted off of the support. There is no significant charge transfer from W to B. When taken off of the substrate, and without being constrained to 2-D, the π-phase has no imaginary phonons, and retains the structure up to 1,800 K, according to Born-Oppenheimer Molecular Dynamics (BOMD). At 1,800 it transforms into the previously reported χ_3 2-D structure. On W(110), the χ_3 is less stable than the π-phase.

The AdNDP analysis of this material (Figure 8D) indicates the presence of both localized covalent, and delocalized bonding elements, as is characteristic of boron in many structural contexts, for example, clusters.[57] The single bonds connecting the wider ribbons and narrower ribbons in the structure are 2c-2e σ-bonds. There 8 delocalized 3c-2e σ-bonds per unit cell, 2 per rhombus and 6 per hexagon. Just 2 3c-2e states per rhombus and 4 electrons occupying them, make the rhombus locally σ-antiaromatic, with the expected Jahn-Teller distortion away from the square. The 6 delocalized σ-states per hexagon are also consistent with the symmetry. Finally, there are 2

delocalized π-bonds, a 4c-2e π-bond on every rhombus, and a 7c-2e π-bond on every hexagon. Hence, both of these units are locally π-aromatic.

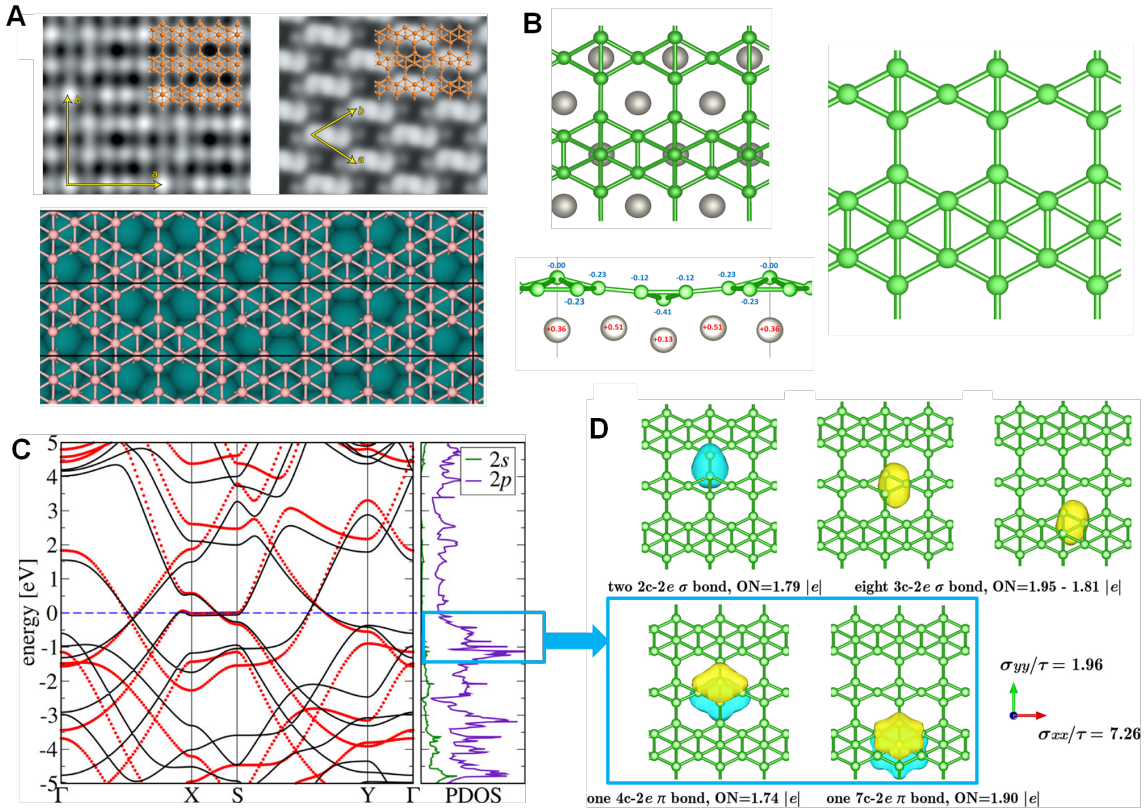

Figure 8. (A) Phases of 2-D boron predicted to exist on Ag (top) and Cu (bottom), with the phases on Ag being experimentally confirmed. (B) The π-phase of 2-D boron predicted to form on W(110): top view, side view with Bader charges shown, and alone, after exfoliation from the W support. (C) The band and DOS plots for the unsupported π-phase; the area near E_F outlines in blue is dominated by 2p-AOs, and corresponds to the localized AdNDP π-states outlined in (D). (D) All AdNDP states: covalent 2c-2e σ-bonds, 3c-2e σ-bonds, and 4c- and 7c- π-bonds. The presence of the π-network of states near E_F, conjugated in the x-direction, and disrupted by covalent σ-bonds in the y-direction, leads to the anisotropy of the conductivity tensor shown at right. Adapted with permissions from Feng, B.; Zhang, J.; Zhong, Q.; Li, W.; Li, S.; Li, H.; Cheng, P.; Meng, S.; Chen, L.; Wu, K. Experimental realization of two-dimensional boron sheets. *Nat. Chem.* **2016**, *8*, 563–568; Mannix, A. J.; Zhou, X. F.; Kiraly, B.; Wood, J. D.; Alducin, D.; Myers, B. D.; Liu, X.; Fisher, B. L.; Santiago, U.; Guest, J. R. Synthesis of borophenes: anisotropic, two-dimensional boron polymorphs. *Science* **2015**, *350*, 1513–1516; Cui, Z.; Jimenez-Izal, E.; Alexandrova, A. N. Prediciton of Two-dimensional Phase of Boron with Anisotropic Electric Conductivity. *J. Phys. Chem. Lett.* **2017**, *8*, 1224-1228.

The most interesting property of the π-phase is specific conductivity. It is metallic, according to the band structure and DOS shown in Figure 8C. Like in graphene, the states near E_F are dominated

by the $2p_z$-AOs on B, but there are many of them at E_F. They are the ones that correspond to the AdNDP π-states just described. The position at E_F taken together with the conjugation of our localized states along the thin and thick ribbons in the structure, indicate that the mechanism of conductivity is through the π-system. It is again the case when π-aromaticity alone, derived from the bonding analysis, does tell us enough about properties. The π-states are obviously very accessible for conductivity, and probably also reactivity.

Because the conjugation of the π-system is interrupted by the single B-B σ-bonds that stitch the ribbons together, we suspected, and then tested, and confirmed that the material is more conducting in the direction of the conjugation. Figure 8D shows the anisotropic conductivity tensor. The conductivity in the x-direction can be further differentially increased or decreased by changing the chemical potential of the electron. Therefore, we predicted a new 2-D material with anisotropic conductivity, a property unique among 2-D materials reported to date. The π-phase is effectively a sheet of covalently linked conducting wires.

3.4.Practical guidelines for constructing a useful cluster representation.

The key to the "divide-and-conquer" analysis is to construct an appropriate cluster model. It is generally not safe to use pure geometric criteria to decide on one. For example, consider SmB_6, which has the cubic unit cell with Sm vertices and an octahedral B_6 cluster inside. An instinct might be to consider Sm atoms interacting with the B_6 octahedron. However, the ELF analysis showed no B-B bonds within B_6.[41] Instead, the B_2 diamers piercing the wall between two neighboring unit cells are bonded, and give rise to more appropriate SmB_2 and Sm_2B_2 cluster models, for the description of Sm-B interactions in this solid. Hence, one way to decide on a cluster model is to use ELF to locate the bonding basins, or QTAIM to locate bond CPs, in the solid. Then, one can proceed to cutting the corresponding bonded cluster out of the solid and analyzing it in isolation. Its geometry has to be optimized, which will necessarily take it away from the optimum seen in the solid. The analysis of chemical bonding in the cluster can be done using all the usual methods of computational molecular chemistry, and spectroscopy. Familiar types of bonds will be discovered, such as σ-, π-, δ-… by type of the overlap, dative, delocalized, ionic, etc. Chemists can associate these bonds with possible properties. This completes the "divide" part of the approach. Next, because clusters have dangling valencies, some bonds (MOs), particularly those near the HOMO-LUMO gap, will be unoccupied in the solid, and therefore will not define any properties. In order to realize which of the bonds exist in

the solid, it is necessary to plot the real-space wave functions, or projected DOS of the solid, particularly near E_F. Several points in the Brullouin zone may need to be analyzed in cases of very convoluted band structures with multiple bands crossings. After that, one can make a one-to-one matching between cluster MOs and Bloch states simply by visual examination, or by projecting the states onto AOs and analyzing the compositions. Thus, the occupied states in the solid can be recognized with the help of clusters, and associated with properties. The "conquer" part is now complete. An alternative approach is AdNDP-based, which would localize the density onto bonds of various possible centerdnesses, matching the symmetry of the lattice. The cluster motifs will thus appear right in the solid state, ready for the usual analysis. In order to connect the AdNDP results with state energies, it is again necessary to plot the real-space wave functions or projected DOS of the solid, and identify the regions in the band structure or DOS to which the localized AdNDP states correspond. With energy information at hand, properties such as reactivity and conductivity resultant from bonding in the embedded cluster motifs can be inferred.

SUMMARY AND OUTLOOK

Through the examples presented in this article, we showed an approach for the analysis of chemical bonding in materials, done by and for chemists, that gives access to understanding, predicting, and designing for interesting functions of materials, such as catalytic selectivity, hardness, conductivity, and magnetism. Though the number of examples is limited so far, the breadth of possible applications is encouraging, with both the microscopic chemical properties and macroscopic physical and mechanical properties having been explored. We therefore feel that this direction is promising and on the rise. The approach is based on considering elementary structural units of the extended system, and mapping the interpretation of bonding back to the solid. The elementary units can be small clusters characterized with the full wealth of theoretical and also experimental spectroscopic methods. The cluster fragmentation approach is often very beneficial, particularly in cases where the electronic structure of the solid is highly complicated and usual computational tools such as Density Functional Theory do not work. The choice for useful cluster motifs needs to be based on the bonding interactions in the solid, detected through the analysis of the charge density, for example. When going from clusters back to the solid state, the valence undersaturation of clusters needs to be taken into account, and the energy information has to be attributed to the realized bonding model. Alternatively, the small units can be realized right in the

solid state, through electron-localization techniques such as AdNDP. In this case too, the energy content needs to be added back to the obtained Lewis-like picture, in order to relate it to properties. In either case, the attractiveness of our "divide-and-concur" approach to the bonding analysis of materials is that it is very visual for chemists. We can use the large body of knowledge accumulated in the chemistry community, e.g. such phenomena as aromaticity, covalency, and back-donation, and the properties that are known to be associated with them. We show specific examples of how understanding of bonding through this prism gave rise to testable predictions of new functional materials.

Finally, we notice that for some of materials properties, it is important to consider the chemical bonding not only in the static fashion for the material in equilibrium, but also as it evolves when the material is exposed to stress or a perturbation related to its practical use. One such example is the mechanical hardness, where bonding under applied mechanical stress needs to be evaluated. Other examples of this sort are, of course, new phases formed only under high pressure, or specific materials used in conditions of applied fields or radiation, though such examples were not considered in the present article.

Overall, we hope to offer the field a lever at materials design that is enabled with chemical intuition.

AUTHOR INFORMATION

Corresponding Author

*A. N. Alexandrova. E-mail: ana@chem.ucla.edu

Notes

The author declares no competing financial interest(s).

Biography

Anastassia Alexandrova is an Associate Professor in the Department of Chemistry and Biochemistry, University of California, Los Angeles. Born and raised in USSR, she received her B.S. and M.S. degrees in chemistry from Saratov University, Russia. She then obtained her Ph.D. in

theoretical physical chemistry in Utah State University in 2005, and was then a Postdoctoral Associate and then American Cancer Society Postdoctoral Fellow at Yale University. She joined the faculty of UCLA in 2010. Anastassia's research is in theory and computation, and design of materials, including catalysis, alloys, and natural and artificial enzymes, and the development of associated multiscale and machine learning modeling methodologies. She is a recipient of numerous awards, such as DARPA Young Faculty Award, Sloan Fellowship, NSF CAREER Award, the Rising Star Award of the WCC American Chemical Society, and UCLA's Glenn T. Seaborg Award, Herbert Newby McCoy Award for excellence in faculty research, and Hanson-Dow Award for Excellence in Teaching. Anastassia currently serves as a Chair of the Theory sub-division of PHYS of the American Chemical Society. Anastassia organizes numerous conferences and symposia around the World, such as the annual International Conference of Chemical Bonding (ICCB), symposia at the national ACS and APS meetings, and the International Conference of Theoretical Aspects of Catalysis (ICTAC).

ACKNOWLEDGEMENTS

This work was supported by the NSF Career Award (No. CHE1351968).

REFERENCES

(1) The Nature of the Chemical Bond and the Structure of Molecules and Crystals: An Introduction to Modern Structural Chemistry. Pauling, L. Cornell University Press; 3rd Ed.; 1960.

(2) Valency and Bonding: A Natural Bond Orbital Donor-Acceptor Perspective. Weinhold, F.; Landes, C. R. Cambridge University Press; 1st Ed.; 2005.

(3) Pauling, L. The Metallic State. *Nature* **1948**, 1019-1020.

(4) Pauling, L. A resonating-valence-bond theory of metals and intermetallic compounds. *Proc. R. Soc. London* **1949**, *196*, 343-362.

(5) Hoffmann, R. How Chemistry and Physics Meet in the Solid State. *Angew. Chem. Int. Ed.* **1987**, *26*, 846–878.

(6) Chemical Bonding in Solids. J. K. Burdett, John Wiley & Sons, Chichester, New York, Weinheim, Brisbane, Singapore, Toronto, 1997, ISBN-13: 978-0471971306.

(7) The Electronic Structure and Chemistry of Solids. P. A. Cox, Clarendon Press, 1987, ISBN-13: 978-0198552048.

(8) Orbital Approach to Electronic Structure of Solids, E. Canadell, M.-L. Doublet, C. Iung, Oxford University Press, Oxford 2012, ISBN 978-0199534937.
(9) Miao, M.-S.; Hoffmann, R.; Botana, J.; Naumov, I. I.; Hemley, R. J. Quasimolecules in Compressed Lithium. *Angew. Chem. Int. Ed.* **2017**, *56*, 972 –975.
(10) Cairns, A. B.; Cliffe, M. J.; Paddison, J. A. M.; Daisenberger, D.; Tucker, M. G.; Coudert, F.-X.; Goodwin, A. L. Encoding complexity within supramolecular analogues of frustrated magnets. *Nat. Chem.* **2016**, *8*, 442-447.
(11) Neilson, J. R.; Morse, D. E.; Melot, B. C.; Shoemaker, D. P.; Kurzman, J. A.; Seshadri, R. Understanding complex magnetic order in disordered cobalt hydroxides through analysis of the local structure. *Phys. Rev. B* **2011**, *83*, 094418.
(12) Kurzman, J. A.; Martinolich, A. J.; Neilson, J. R. Influence of interstitial Mn on local structure and magnetism in $Mn_{1+\delta}Sb$. *Phys. Rev. B.* **2015**, *92*, 184414.
(13) Overy, A. R.; A. B.; Cliffe, M. J.; Simonov, A.; Tucker, M. G.; Goodwin, A. L. Design of crystal-like aperiodic solids with selective disorder–phonon coupling. *Nat. Comm.* **2015**, *7*, 10445.
(14) Vinokur, A. I.; Fredrickson, D. C. 18-Electron Resonance Structures in the BCC Transition Metals and Their CsCl-type Derivatives. *Inorg. Chem*. **2017**, *56*, 2834−2842.
(15) Vinokur, A. I.; Fredrickson, D. C. Toward Design Principles for Diffusionless Transformations: The Frustrated Formation of Co−Co Bonds in a Low-Temperature Polymorph of $GdCoSi_2$. *Inorg. Chem.* **2016**, *55*, 6148−6160.
(16) Yannello, V. J.; Kilduff, B. J.; Fredrickson, D. C. Isolobal Analogies in Intermetallics: The Reversed Approximation MO Approach and Applications to $CrGa_4$- and Ir_3Ge_7-Type Phases. *Inorg. Chem.* **2014**, *53*, 2730–2741.
(17) Alidousta, N.; Carter, E. A. First-principles assessment of hole transport in pure and Li-doped NiO. *Phys. Chem. Chem. Phys.* **2015**, *17*, 18098-18110.
(18) Eberhart, M. E. Are metals made from molecules? *Struct. Chem.* **2017**, DOI: 10.1007/s11224-017-0917-z.
(19) Bader, R. F. W. Atoms in Molecules: A Quantum Theory; Oxford University Press: Oxford, U.K., 1990.
(20) Becke, A. D.; Edgecombe, K. E. A simple measure of electron localization in atomic and molecular systems. *J. Chem. Phys*. **1990**, *92*, 5397-5403.

(21) *NBO 5.0.* Glendening, E. D.; Badenhoop, J, K.; Reed, A. E.; Carpenter, J. E.; Bohmann, J. A.; Morales, C. M.; Weinhold, F. Theoretical Chemistry Institute, University of Wisconsin, Madison (2001).
(22) Zubarev, D. Yu.; Boldyrev, A. I. Developing paradigms of chemical bonding: adaptive natural density partitioning. *Phys. Chem. Chem. Phys*., **2008**, *10*, 5207-5217.
(23) Galeev, T. R.; Dunnington, B. D.; Schmidt, J. R.; Boldyrev, A. I. Solid state adaptive natural density partitioning: a tool for deciphering multi-center bonding in periodic systems *Phys. Chem. Chem. Phys*. **2013**, *15*, 5022-5029.
(24) Popov, I. A.; Bozhenko, K. V.; Boldyrev, A. N. Is Graphene Aromatic? *Nano Research* **2012**, *5*, 117-123.
(25) Yang, L.-M.; Bačić, V.; Popov, I. A.; Boldyrev, A. I.; Heine, T.; Frauenheim, T.; Ganz, E. Two-dimensional Cu_2Si Monolayer with Planar Hexacoordinate Copper and Silicon Bonding. *J. Am. Chem. Soc*. **2015**, *137*, 2757-2762.
(26) Nandula, A.; Trinh, Q. T.; Saeys, M.; Alexandrova, A. N. Origin of Extraordinary Stability of Square Planar Carbon in Surface Carbides of Co and Ni, and Beyond. *Angew. Chem. Int. Ed.* **2015**, *54*, 5312-5316.
(27) Tan; K. F.; Chang. J.; Borgnab, A.; Saeys, M. Effect of boron promotion on the stability of cobalt Fischer–Tropsch catalysts. *J. Catal*. **2011**, *280*, 50-59.
(28) Xu, J.; Saeys, M. First Principles Study of the Effect of Carbon and Boron on the Activity of a Ni Catalyst. *J. Phys. Chem. C* **2009**, *113*, 4099–4106.
(29) Jimenez-Izal, E.; Saeys, M.; Alexandrova, A. N. Metallic and Magnetic 2D Materials Containing Planar Tetracoordinated C and N. *J. Phys. Chem. C* **2016**, *120*, 21685-21690.
(30) Li, X.; Zhang, H.-F.; Wang, L.-S.; Geske, G. D.; Boldyrev, A. I. Pentaatomic Tetracoordinate Planar Carbon, $[CAl_4]^{2-}$: A New Structural Unit and Its Salt Complexes. *Angew. Chem., Int. Ed*. **2000**, *39*, 3630-3632.
(31) Alexandrova, A. N.; Nayhouse, M. J.; Huynh, M. T.; Kuo, J. L.; Melkonian, A. V.; Chavez, G. De J.; Hernando, N. M.; Kowal, M. D.; Liu, C.-P. Selected $AB_4^{2-/-}$ (A = C, Si, Ge; B = Al, Ga, In) Ions: A Battle between Covalency and Aromaticity, and Prediction of Square Planar Si in $SiIn_4^{2-/-}$. *Phys. Chem. Chem. Phys.* **2012**, *14*, 14815-14821.
(32) Chung, H.; Weinberger, M.; Levine, J.; Kavner, A.; Yang, J.; Tolbert, S.; Kaner, R. Synthesis of ultra-incompressible superhard rhenium diboride at ambient pressure. *Science* **2007**, *316*, 436-439.

(33) Cumberland, R.; Weinberger, M.; Gilman, J.; Clark, S.; Tolbert, S.; Kaner, R. Osmium Diboride, An Ultra-Incompressible, Hard Material. *J. Am. Chem. Soc.* **2005**, *127*, 7264-7265.
(34) Kaner, R.; Gilman, J.; Tolbert, S. Designing superhard materials. *Science* **2005**, *308*, 1268-1269.
(35) Lech, A.; Turner, C.; Mohammadi, R.; Tolbert, S.; Kaner, R. Structure of superhard tungsten tetraboride: A missing link between MB_2 and MB_{12} higher borides. *Proc. Natl. Acad. Sci. U.S.A.* **2015**, *112*, 3223-3228.
(36) Richards, S. M.; Kaspar J. S. The crystal structure of YB_{66}. *Acta Cryst*. **1969**, *B25*, 237-251.
(37) Kang, W. N.; Kim, H.-J.; Choi, E.-M.; Jung, C. U.; Lee, S.-I. MgB_2 Superconducting Thin Films with a Transition Temperature of 39 Kelvin. *Science* **2001**, *292*, 1521-1523.
(38) Fokwa, B. P. T.; Samolyuk, G. D.; Miller, G. J.; Dronskowski, R. Ladders of a Magnetically Active Element in the Structure of the Novel Complex Boride $Ti_9Fe_2Ru_{18}B_8$: Synthesis, Structure, Bonding, and Magnetism. *Inorg. Chem.* **2008**, *47*, 2113–2120.
(39) Cooley, C.; Aronson, M.; Fisk, Z.; Canfield, P. SmB_6 - Kondo Insulator Or Exotic Metal *Phys. Rev. Lett.* **1995**, *74*, 1629–1632.
(40) Neupane, M.; Alidoust, N.; Xu, S.; Kondo, T.; Ishida, Y.; Kim, D.-J.; Liu, C.; Belopolski, I.; Jo, Y.; Chang, T.-R. Surface Electronic Structure Of The Topological Kondo-Insulator Candidate Correlated Electron System SmB_6 *Nat. Commun*. **2013**, *4*, 2991.
(41) SmB_6^- Cluster Anion: Covalency Involving f-Orbitals. Robinson, P. J.; Zhang, X.; McQueen, T. M.; Bowen, K. H.; Alexandrova, A. N. *J. Phys. Chem. A* **2017**, *121*, 1849-1854.
(42) Romanescu, C.; Galeev, T. R.; Li, W.-L.; Boldyrev, A. I.; Wang, L.-S. Transition-Metal-Centered Monocyclic Boron Wheel Clusters (MB_n): A New Class of Aromatic Borometallic Compounds. *Acc. Chem. Res*. **2013**, *46*, 350-358.
(43) Carenco, S.; Portehaul, D.; Boissière, C.; Mézailles, C.; Sanchez, C. Nanoscaled Metal Borides and Phosphides: Recent Developments and Perspectives. *Chem. Rev*. **2013**, *113*, 7981–8065.
(44) Grant, J. T.; Carrero, C. A.; Goeltl, F.; Venegas, J.; Mueller, P.; Burt, S. P.; Specht, S. E.; McDermott, W. P.; Chieregato, A.; Hermans, I. Selective Oxidative Dehydrogenation of Propane to Propene using Boron Nitride Catalysts. *Science* **2016**, *354*, 1570-1573.
(45) Dadras, J.; Jimenez-Izal, E.; Alexandrova, A. N. Alloying Pt Sub-Nano-Clusters with Boron: Sintering Preventative and Coke Antagonist? *ACS Catal.* **2015**, *5*, 5719-5727.

(46) Ha, M.-A.; Baxter, E. T.; Cass, A. C.; Anderson, S. L.; Alexandrova, A. N. Boron Switch for Selectivity of Catalytic Dehydrogention on Size-Selected Pt Clusters on Al_2O_3. *J. Am. Chem. Soc.* **2017**, *139*, 11568-11575.
(47) Robinson, P. J.; Liu, G.; Ciborowski, S.; Martinez-Martinez, C.; Chamorro, J.; McQueen, T. M.; Bowen, K. H.; Alexandrova, A. N. Mystery of Three Borides: Promiscuous Metal-Boron Bonding Governing Superhard Structures. **2017**, submitted.
(48) Tang, H.; Ismail-Beigi, S. Novel precursors for boron nanotubes: the competition of two-center and three-center bonding in boron sheets *Phys. Rev. Lett.* **2007**, *99*, 115501– 115504.
(49) Tang, H.; Ismail-Beigi, S. Self-doping in boron sheets from first principles: A route to structural design of metal boride nanostructures *Phys. Rev. B: Condens. Matter Mater. Phys.* **2009**, *80,* 134113–134121.
(50) Özdoğan, C.; Mukhopadhyay, S.; Hayami, W.; Güvenç, Z. B.; Pandey, R.; Boustani, I.The unusually stable B100 fullerene, structural transitions in boron nanostructures, and a comparative study of α- and γ-boron and sheets *J. Phys. Chem. C* **2010**, *114*, 4362– 4375.
(51) Wu, X.; Dai, J.; Zhao, Y.; Zhuo, Z.; Yang, J.; Zeng, X. C. Two-dimensional boron monolayer sheets. *ACS Nano* **2012**, *6*, 7443– 7453.
(52) Penev, E. S.; Kutana, A.; Yakobson, B. I. Can Two-Dimensional Boron Superconduct? *Nano Let.* **2016**, *16*, 2522-2526.
(53) Tai, G.; Hu, T.; Zhou, Y.; Wang, X.; Kong, J.; Zeng, T.; You, Y.; Wang, Q. Synthesis of atomically thin boron films on copper foils. *Angew. Chem., Int. Ed.* **2015**, *54*, 15473–15477.
(54) Feng, B.; Zhang, J.; Zhong, Q.; Li, W.; Li, S.; Li, H.; Cheng, P.; Meng, S.; Chen, L.; Wu, K. Experimental realization of two-dimensional boron sheets. *Nat. Chem.* **2016**, *8*, 563–568.
(55) Mannix, A. J.; Zhou, X. F.; Kiraly, B.; Wood, J. D.; Alducin, D.; Myers, B. D.; Liu, X.; Fisher, B. L.; Santiago, U.; Guest, J. R. Synthesis of borophenes: anisotropic, two-dimensional boron polymorphs. *Science* **2015**, *350*, 1513–1516.
(56) Cui, Z.; Jimenez-Izal, E.; Alexandrova, A. N. Prediciton of Two-dimensional Phase of Boron with Anisotropic Electric Conductivity. *J. Phys. Chem. Lett.* **2017**, *8*, 1224-1228.
(57) Alexandrova, A. N.; Boldyrev, A. I.; Zhai, H.-J.; Wang, L.-S. All-Boron Aromatic Clusters as Potential New Inorganic Ligands and Building Blocks in Chemistry. *Coord. Chem. Rev.* **2006**, *250*, 2811-2866.

TOC Graphics: